Analysis of an Aerotorquer for the Control of CubeSats with Large Torque Requirements

AE 8900 MS Special Problems Report
Lightsey Research Group (LRG)
Space Systems Design Lab (SSDL)
Guggenheim School of Aerospace Engineering
Georgia Institute of Technology

Author:
Matthew R. Heron

Advisor:
Prof. E. Glenn Lightsey

April 27, 2018

Analysis of an Aerotorquer for the Control of CubeSats with Large Torque Requirements

Matthew Heron* and E. Glenn Lightsey†
Georgia Institute of Technology, Atlanta, GA, 30332

Traditionally, Earth-pointing CubeSats have Attitude Control Systems (ACS) that consist of two primary types of actuators – reaction wheels and magnetorquers. Reaction wheels provide the fine attitude control while the magnetorquers prevent reaction wheel saturation. This control scheme may not always meet CubeSat mission requirements, however, for some missions require a spacecraft with a large angular momentum (e.g. CubeSats with spinning instruments). In this case, the gyroscopic stiffness induced by the angular momentum will impose large torque requirements on the ACS to maintain Earth-pointing. This torque requirement on the reaction wheels may cause the wheels to spin up to saturation before the magnetorquers can unload the reaction wheel momenta. This paper analyzes the ACS feasibility and design of a 12U dual-spinning, nadir-pointing satellite. Two distinct ACS schemes are considered. In the first control scheme, the embedded angular momentum of the satellite is offset by a momentum wheel. In the second scheme, the use of an aerotorquer (i.e. drag panel) to provide the required torque is considered.

Nomenclature

$\boldsymbol{e}_i$	=	i^{th} Euclidean basis unit vector in 3-dimensional space
$\mathfrak{I}$	=	identity matrix
A_{DP}	=	surface area of aerotorquer
C_D	=	coefficient of drag of the aerotorquer
$\boldsymbol{F}_{DP}$	=	force of drag on aerotorquer
F_{BIT-3}	=	nominal force of Busek BIT-3 Ion Thruster
ρ_{avg}	=	average air density the spacecraft experiences at a given orbital altitude
P	=	orbital period of the spacecraft
v	=	speed of the spacecraft relative to an Earth-Centered Inertial (ECI) frame

Notation

${}^{A}\boldsymbol{B}$	=	magnetic field vector with respect to reference frame A
${}^{B}\boldsymbol{h}_A$	=	angular momentum vector of the section of the spacecraft represented by A expressed in the coordinates of reference frame B
$[I_B^A]_C$	=	inertia of the section of the spacecraft represented by A relative to the origin of the B frame using the basis vectors of the C frame
m_A	=	mass of the section of the spacecraft represented by A
${}^{B}\theta_i^A$	=	angular displacement of the i^{th} axis of reference frame A with respect to the i^{th} axis of reference frame B
$\boldsymbol{r}_{A/B}$	=	position vector from the origin of the B frame to the origin of the A frame
${}^{A}\hat{\boldsymbol{\tau}}_X$	=	commanded torque of component X expressed in reference frame A
${}^{B}\boldsymbol{\omega}^A$	=	angular momentum vector of reference frame A with respect to reference frame B
$x \equiv \|\boldsymbol{x}\|_2$	=	2-norm of the vector $\boldsymbol{x}$

* Graduate Student, Guggenheim School of Aerospace Engineering, Georgia Tech, mheron3@gatech.edu
† Professor, Guggenheim School of Aerospace Engineering, Georgia Tech, glenn.lightsey@gatech.edu

I. Introduction

The Attitude Control System (ACS) actuators of small satellites are limited by both size and power. Traditionally, CubeSats are controlled via a combination of reaction wheels and magnetorquers[1]. Reaction wheels spin up and down to impose reaction torques on the spacecraft. These actuators typically provide the fine pointing control of small satellites. Nevertheless, they are susceptible to momentum buildup due to attitude perturbations (e.g. atmospheric drag, zonal harmonics, etc.) which can lead to actuator saturation. Magnetorquers produce torques on the spacecraft in the direction normal to the plane formed by the local magnetic field and the magnetorquer magnetic dipole. When applied to spacecraft ACS with reaction wheels, they can be used for unloading the momentum built up in the reaction wheels[2]. The actuators required for attitude control are highly dependent on the mass properties of the spacecraft and the pointing requirements. Li, Post, Wright, and Lee present two distinct control schemes for a 1U CubeSat of uniform mass distribution[3]. The first ACS scheme uses three reaction wheels. The second control scheme relies on three magnetorquers and one reaction wheel. They successfully verify the performance of the controllers through detumble mode, limb pointing mode, and nadir pointing mode. Psiaki proves the stability of a magnetorquer-only attitude control system using an Asymptotic Periodic Linear Quadratic Regular (LQR) controller[2]. This research applies for spacecraft with relatively relaxed pointing requirements of 0.1 to 1.0 degree error.

More stringent pointing requirements and/or more challenging spacecraft designs can require ACS solutions that deviate from the traditional control scheme. One such challenge is the requirement that the science instrument is spinning at some angular rate while constantly precessing the attitude with respect to an inertial frame (e.g. the requirements of a nadir-pointing, dual-spinning spacecraft). The embedded angular momentum induces gyroscopic stiffness which increases the torque required to precess the angular momentum vector[1]. Neilsen, Weston, Fish, and Bingham present a control scheme for the dual-spinning DICE mission[4]. With moderate angular momentum requirements and relaxed pointing requirements, they meet their objectives with a magnetorquer-only control scheme. Wise et al. propose a control scheme for the dual-spinning 2U CubeSat MicroMAS. Their control scheme requires three reaction wheels and three magnetorquers for ACS actuation[1,5].

This paper considers two potential ACS schemes for nadir-pointing spacecraft with significantly larger inertias than DICE or MicroMAS and more stringent pointing requirements. In the first scheme, a momentum wheel is used to create a zero-momentum state. In addition, reaction wheels are used to precess the spin axis to maintain nadir pointing, and magnetorquers are used for momentum unloading. In the second scheme, a drag panel is used to provide the torque required to overcome the gyroscopic stiffness, reaction wheels are used to precess the spin axis to maintain nadir pointing, magnetorquers are used for momentum unloading, and two ion thrusters are used to cancel the component of the drag panel torque imposed on the satellite that induces an angular momentum normal to the desired angular momentum. The Aerospace Corporation presents an ACS scheme for the 1U AeroCube-4 CubeSats that successfully implements variable-angle drag panels for attitude control and orbit adjustments[6]. These 1U satellites were not dual-spinners, however, so they did not have to overcome dynamics due to gyroscopic stiffness.

II. Problem Statement

This paper considers the attitude control of a 12U ($20\ cm \times 20\ cm \times 30\ cm$) dual-spinning spacecraft in a circular Low-Earth Orbit (LEO) that is required to maintain nadir-pointing. The following ACS requirements are considered:

1. The instrument (and the top 6U of the spacecraft) must be rotating at 18 RPM ($\pm$ 0.1 RPM) with respect to the Local-Vertical-Local-Horizontal (LVLH) frame.
2. The 12U spacecraft bus must be nadir-pointing to within 0.5 degrees (SSE of pointing error and attitude estimation error).

To meet these requirements, the instrument and half of the 12U bus will be assumed to be rotating at required rotation rate while keeping the second half of the bus, including the ACS components non-rotating (NR) with respect to the LVLH frame. The ACS will be comprised of the following actuators:

- Reaction Wheels (3) – Sinclair, 0.03 N·m·s
- Magnetorquers (3) – 0.5 A·m²

Two control schemes are considered. In the first scheme, the non-rotating section of the bus houses a Blue Canyon 4.0 N·m·s momentum wheel. In the second scheme, a flat drag panel lowers the spacecraft center of pressure,

effectively providing the torque required to keep the spacecraft nadir-point (i.e. rotating at 1 revolution per orbit). In addition to the drag panel, two Busek BIT-3 ion thrusters are used for this control scheme.

To verify that the ACS design and control laws meet the requirements stated above, a spacecraft simulation was developed to model the orbit and attitude of a 12U dual-spinning spacecraft under all significant environmental torques (i.e. drag, zonal harmonics, gravity gradient, and solar radiation pressure).

These analyses prove the feasibility of the attitude control in science mode. Further analyses must be performed to verify detumble, system checkout mode, safe mode, and spin-up mode.

III. Reference Frames

Table I shows all relevant reference frames for the problem statement described in *Section II*.

Table I. ACS Reference Frames

Reference Frame	Description
N	Earth-Centered Inertial Frame
L	Local-Vertical-Local-Horizontal Frame
NR	Non-Rotating Bus Frame
R	Rotating Bus Frame
A	Instrument/ Feed Frame
RW_i	i^{th} Reaction Wheel Frame
MT_i	i^{th} Magnetorquer Frame
W	Momentum Wheel Frame
DP	Drag Panel Reference Frame
T_i	i^{th} Ion Thruster Frame
SC	Spacecraft Reference Frame

As stated, the spacecraft has a circular orbit and the non-rotating section of the dual-spinner will be aligned with the LVLH frame. Therefore, the control system must align the NR frame with the L frame. Note that the A frame is aligned with the R frame. The desired rotation rate of the R frame with respect to the NR frame is the following:

$$ {}^{NR}\boldsymbol{\omega}^{R} = \begin{bmatrix} 0 \\ 0 \\ 18 \pm 0.1 \end{bmatrix} RPM \tag{1} $$

Note the following notation:

$$ {}^{NR}\omega^{R} \equiv \left\| {}^{NR}\boldsymbol{\omega}^{R} \right\|_2 \tag{2} $$

The origin of the R frame is the center of mass of the rotating section of the bus, excluding the mass of the rotating instrument. The origin of the NR frame is the center of mass of the non-rotating section of the bus. The origin of the A frame is the center of mass of the deployed instrument.

The origins of the RW_i, MT_i, W, and T_i, frames are the centers of mass of the i^{th} reaction wheel, the i^{th} magnetorquer, momentum wheel, and the i^{th} ion thruster, respectively. The RW_i and MT_i frames are aligned such that the z-axis of the RW_i and MT_i frames are aligned with the i^{th} axis of the NR frame (which is nominally aligned with the L frame). The z-axis of the T_1 and T_2 frames are aligned with the positive and negative x-axes, respectively. The W frame is aligned with the NR frame. It is important to note that this implies that the spin axis of the momentum wheel is aligned with the spin axis of the rotating section of the dual-spinner.

The origin of the DP reference frame is the center of mass (i.e. geometric center, assuming a uniformly distributed drag panel) of the aerotorquer. The z-axis of the DP frame is aligned with the z-axis of the NR frame. The x-axis of the DP frame is normal to the large surface area of the drag panel. Note that the x- and y- axes of the DP frame are rotated by ${}^{NP}\theta_1^{DP}$ from the x- and y- axes of the NR frame. Therefore, there are components of the aerotorquer's

normal vector (i.e. drag unit vector) in both the x- and y- direction of the NR frame. In the following sections of this paper, ${}^{NP}\theta_1^{DP}$ is referred to as the angle of attack of the aerotorquer.

The origin of the SC reference frame is the center of mass of the entire spacecraft. Its basis vectors align with the basis vectors of the NR frame.

IV. Moment of Inertia Approximation

The spacecraft inertia can be represented as follows:

$$[I_{A+R}^{A+R}]_R = [I_{A+R}^{A}]_R + [I_{A+R}^{R}]_R \tag{3}$$

where

$$[I_{A+R}^{A}]_R = [I_A^A]_A + m_A \cdot \left[\left\|\boldsymbol{r}_{(A+R)/A}\right\|^2 \Im - \boldsymbol{r}_{(A+R)/A}\boldsymbol{r}_{(A+R)/A}^T\right] \tag{4}$$

$$[I_{A+R}^{R}]_R = [I_R^R]_R + m_R \cdot \left[\left\|\boldsymbol{r}_{(A+R)/R}\right\|^2 \Im - \boldsymbol{r}_{(A+R)/R}\boldsymbol{r}_{(A+R)/R}^T\right] \tag{5}$$

The following parameters were assumed for the rotating instrument:

$$[I_A^A]_A = \begin{bmatrix} 2.5 & 0.0 & 0.0 \\ 0.0 & 2.5 & 0.0 \\ 0.0 & 0.0 & 1.5 \end{bmatrix} kg \cdot m^2 \tag{6}$$

$$\boldsymbol{r}_{R/A} = \begin{bmatrix} 0.0 \\ 0.0 \\ -0.5 \end{bmatrix} m \tag{7}$$

The inertias of the non-rotating section and rotating section were approximated to be uniform mass distributions of $1.5kg$ and $10.0kg$, respectively. The calculations are as follows:

$$[I_R^R]_R = \left(\frac{m_R}{12}\right) \cdot \begin{bmatrix} (h_R^2 + w_R^2) & 0 & 0 \\ 0 & (d_R^2 + h_R^2) & 0 \\ 0 & 0 & (w_R^2 + d_R^2) \end{bmatrix} = \begin{bmatrix} 0.008 & 0.000 & 0.000 \\ 0.000 & 0.008 & 0.000 \\ 0.000 & 0.000 & 0.010 \end{bmatrix} kg \cdot m^2 \tag{8}$$

$$[I_{NR}^{NR}]_{NR} = \left(\frac{m_{NR}}{12}\right) \cdot \begin{bmatrix} (h_{NR}^2 + w_{NR}^2) & 0 & 0 \\ 0 & (d_{NR}^2 + h_{NR}^2) & 0 \\ 0 & 0 & (w_{NR}^2 + d_{NR}^2) \end{bmatrix} = \begin{bmatrix} 0.052 & 0.000 & 0.000 \\ 0.000 & 0.052 & 0.000 \\ 0.000 & 0.000 & 0.067 \end{bmatrix} kg \cdot m^2 \tag{9}$$

Finally, the inertia of the instrument and rotating bus with respect to the center of mass of the combined system is the following:

$$[I_{A+R}^{A+R}]_R = \begin{bmatrix} 2.879 & 0.000 & 0.000 \\ 0.000 & 2.879 & 0.000 \\ 0.000 & 0.000 & 1.577 \end{bmatrix} kg \cdot m^2 \tag{10}$$

V. ACS Design – Momentum Wheel

The momentum wheel, aligned with the spin axis of the instrument, rotates in the opposite direction of the top portion of the bus to cancel the net angular momentum of the spacecraft. This eliminates the large torque requirements on the rest of the ACS that results from attempting to precess a large angular momentum vector to maintain nadir-pointing. The momentum wheel will spin at a *constant* rate such that the angular momentum of the wheel cancels the *nominal* angular momentum of the rotating portion of the bus:

$$^{NR}\boldsymbol{h}_W = -^{NR}\bar{\boldsymbol{h}}_R \tag{11}$$

$^{NR}\boldsymbol{h}_W$ is the angular momentum vector of momentum wheel expressed in non-rotating bus coordinates. $^{NR}\bar{\boldsymbol{h}}_R$ is the nominal angular momentum vector (assuming 18 RPM rotation rate) of the rotating bus and instrument expressed in non-rotating bus coordinates.

The reaction wheels provide the fine attitude control necessary to ensure that the system maintains stability and pointing performance that meets that pointing requirement stated above. Each reaction wheel will be governed by the following SISO control law:

$$^{L}\hat{\boldsymbol{\tau}}_{RW_i} = [K_{p_i} \cdot {}^{L}q_i^{NR} + K_{d_i} \cdot {}^{L}\omega_i^{NR} + K_c \cdot ({}^{L}\boldsymbol{\omega}^{NR} \times {}^{L}\boldsymbol{h}_{NR+R+A})_i] \cdot \boldsymbol{e}_i \tag{12}$$

$^{L}\hat{\boldsymbol{\tau}}_{RW_i}$ is the commanded torque of the i^{th} reaction wheel with respect to the LVLH frame. $\boldsymbol{e}_i$ is the i^{th} Euclidean basis unit vector in 3-dimensional space. $^{L}q_i^{NR}$ is the i^{th} component of the quaternion between the non-rotating bus frame and the LVLH frame. $^{L}\omega_i^{NR}$ is the angular rate of the i^{th} axis of the non-rotating bus frame with respect to the i^{th} axis of the LVLH frame. Note that when expressed in the non-rotating bus frame, the spin axis of the i^{th} reaction wheel is aligned with the i^{th} basis vector of the LVLH frame. $^{L}\boldsymbol{h}_{NR+R+A}$ is the net angular momentum of the spacecraft with respect to the LVLH frame.

The magnetorquers prevent reaction wheel saturation that would result from a build-up of momentum due to attitude perturbations. These actuators are governed by the following proportional control law:

$$^{L}\hat{\boldsymbol{\tau}}_{MT_i} = K_{unload} \cdot \left[({}^{L}\boldsymbol{h}_{RW_i} - {}^{L}\hat{\boldsymbol{h}}_{RW_i}) \times {}^{L}\boldsymbol{B}\right] \tag{13}$$

$^{L}\hat{\boldsymbol{\tau}}_{MT_i}$is the commanded torque of the i^{th} magnetorquer with respect to LVLH frame. $^{L}\boldsymbol{h}_{RW_i}$ is the angular momentum of the i^{th} reaction wheel with respect to the LVLH frame. $^{L}\hat{\boldsymbol{h}}_{RW_i}$ is the commanded angular momentum of the i^{th} reaction wheel with respect to the LVLH frame. $^{L}\boldsymbol{B}$ is the magnetic field vector with respect to the LVLH frame.

The motor spinning the rotating portion of the spacecraft is governed by the following control law:

$$\hat{\tau}_{motor} = K_{motor} \cdot ({}^{NR}\omega^{R} - \omega_{des}) \tag{14}$$

$\hat{\tau}_{motor}$ is the commanded torque by the motor. $^{NR}\omega^{R}$ is the rotation rate of the rotating bus frame with respect to the non-rotating bus frame. ω_{des} is the desired rotation rate, 18 RPM.

VI. ACS Design – Aerotorquer with Ion Thrusters

A. Aerotorquer

In this paper, the aerotorquer is a constant-area rectangular panel that applies the torque required to maintain nadir pointing. The other ACS components (i.e. reaction wheels and magnetorquers) perform the fine attitude control. The drag panel area is chosen such that nadir pointing is maintained for the *nominal* angular momentum. This implies that in this design, perturbations to the nominal spacecraft angular momentum are handled via the reaction wheels and magnetorquers instead of the aerotorquer.

The torque required to maintain nadir pointing is derived as follows:

$$\boldsymbol{\tau}_{req} = {}^{ECI}\boldsymbol{\omega}^{NR} \times {}^{NR}\boldsymbol{h}_R \approx \frac{2\pi}{P}\boldsymbol{e}_2 \times {}^{NR}h_R\,\boldsymbol{e}_3 = \frac{2\pi \cdot {}^{NR}h_R}{P}\boldsymbol{e}_1 \tag{15}$$

where P is the orbital period of the spacecraft.

The torque provided by the aerotorquer is approximated as follows:

$$\boldsymbol{\tau}_{DP} = \boldsymbol{r}_{DP/SC} \times \boldsymbol{F}_{DP} \approx \frac{1}{2}\rho_{avg} v^2 C_D r_{DP/SC} \sin {}^{NP}\theta_1^{DP} \left(A_{DP} \sin {}^{NP}\theta_1^{DP} \boldsymbol{e}_1 + A_{DP} \cos {}^{NP}\theta_1^{DP} \boldsymbol{e}_2\right) \quad (16)$$

where ρ_{avg} is the average air density the spacecraft experiences at a given orbital altitude, v is the speed of the spacecraft relative to an Earth-Centered Inertial (ECI) frame, and C_D is the coefficient of drag of the aerotorquer. ${}^{NP}\theta_1^{DP}$ is the angle between the spacecraft velocity vector and the y-axis of the aerotorquer (i.e. the angle of attack of the drag panel).

In future analyses, the angular velocity state of the spacecraft should be estimated. Then, the spacecraft angular momentum of the spacecraft can be estimated using inertia approximations. Finally, the drag panel area can be varied in feedback control via flaps on the panel to account for deviations to the nominal spacecraft angular momentum.

B. Ion Thrusters

From (16), one can see that there is a component of the torque provided in $\boldsymbol{e}_2$ (i.e. y-direction of the NR frame). Left alone, this torque would induce an angular velocity in the x-direction of the NR frame. The ACS components would quickly saturate attempting to correct for this torque.

Therefore, 2 Busek BIT-3 ion thrusters are used to provide a constant torque that cancels the nominal drag panel torque in $\boldsymbol{e}_2$ as follows:

$$F_{BIT-3}(r_{T_1/SC} + r_{T_2/SC}) \approx \frac{1}{2}\rho_{avg} v^2 C_D r_{DP/SC} A_{DP} \sin {}^{NP}\theta_1^{DP} \cos {}^{NP}\theta_1^{DP} \quad (17)$$

Note that (17) is derived assuming the two ion thrusters are placed such that the torque imposed on the spacecraft by each thruster is positive. The two thrusters must be placed such that their thrust vectors are anti-parallel ($\boldsymbol{e}_1$ and -$\boldsymbol{e}_1$). That ensures that the net force on the spacecraft due to the two thrusters is zero. Note that one thruster must be placed above the spacecraft center of mass and the other thruster must be placed below the spacecraft center of mass to ensure that the torque produced is positive.

VII. Spacecraft Simulation and Results

A. Spacecraft Simulation

To verify the ACS design, an orbit and attitude simulation was developed using the NASA-developed spacecraft simulation software "42". This simulation models the attitude of a 12U dual-spinning spacecraft under the following perturbations:

- Drag
- Zonal Harmonics
- Gravity Gradient
- Solar Radiation Pressure

The pointing performance of the spacecraft as well as ACS actuator performance was evaluated over a 72-hour period. Figure 1 shows the simulated nadir-pointing, 12U dual-spinner in the momentum wheel control scheme.

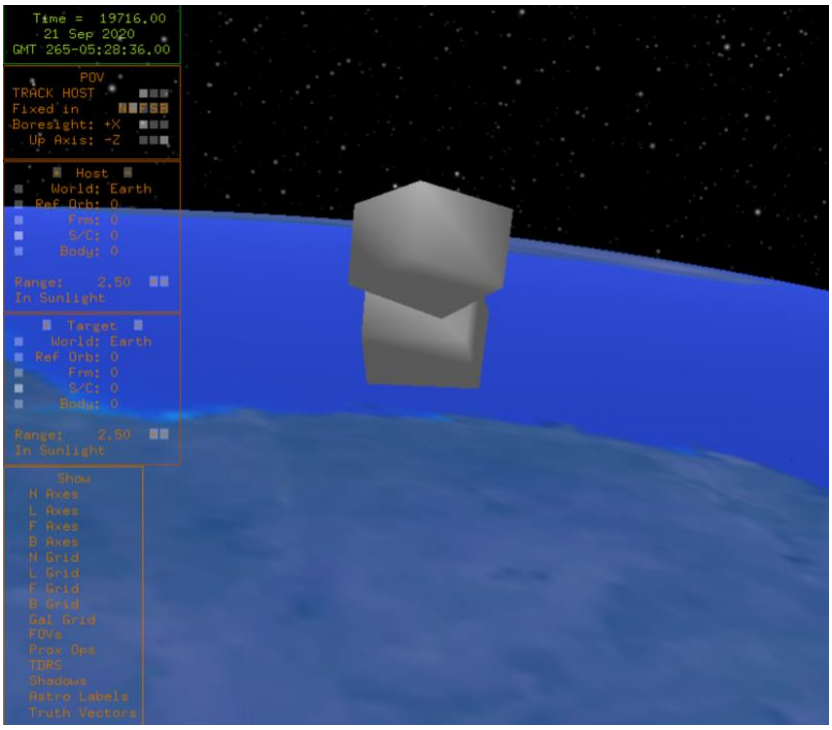

Figure 1. "42" simulation of a 12U dual-spinning spacecraft

B. Traditional Small Satellite ACS

Traditional CubeSat ACS consists of reaction wheels to provide the fine ACS and magnetorquers to prevent wheel saturation in the presence of attitude perturbations. Figures 2, 3, and 4 show the reaction wheel momenta, the magnetorquer magnetic moments, and the angular rate over time. Note that the reactions wheels saturate in less than two minutes. This demonstrates the need for unique ACS solutions.

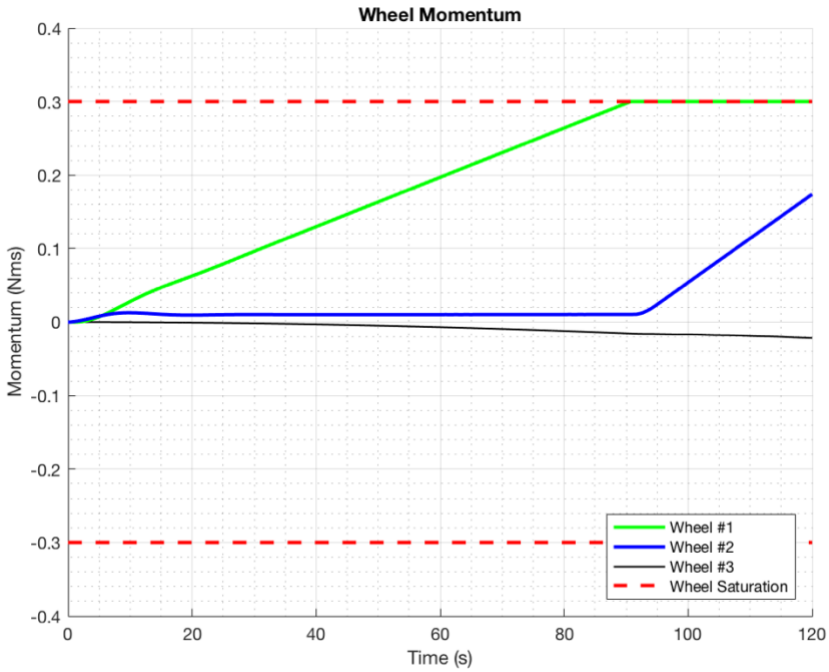

Figure 2. Traditional ACS Control Scheme – Reaction Wheel Momenta vs. Time

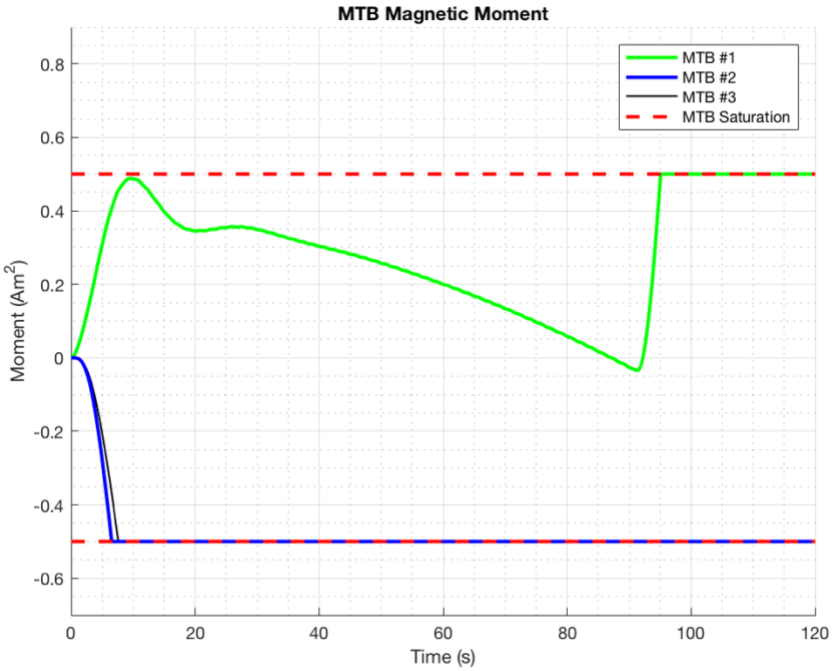

Figure 3. Traditional ACS Control Scheme – Magnetorquer Magnetic Moment vs. Time

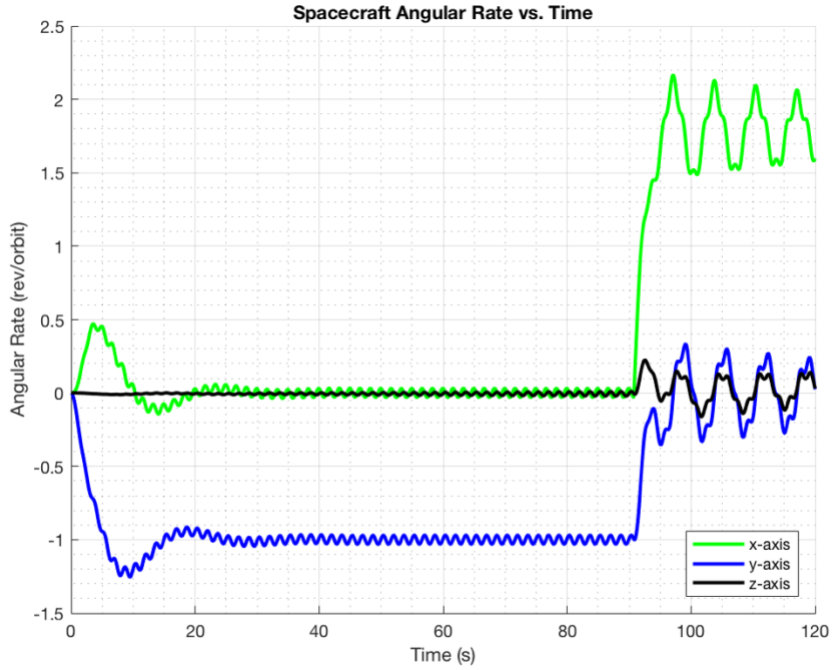

Figure 4. Traditional ACS Control Scheme – Spacecraft Angular Rates vs. Time

C. Momentum Wheel Control Scheme

The pointing performance of the spacecraft as well as ACS actuator performance was evaluated using the spacecraft simulation discussed in *Section IV* over a 72-hour period.

The pointing performance of the spacecraft can be seen in Figure 5. The pointing error of the spacecraft spin axis relative to nadir is less than 0.25 degrees. Assuming the coupling between the estimation uncertainty and the pointing performance is negligible, one can approximate the total error as follows:

$$e_{total}^2 \approx e_{estimation}^2 + e_{pointing}^2 \tag{15}$$

where $e_{estimation}$ is the deviation in the absolute value of the difference between the z-axis estimated attitude state and the z-axis of the actual state, $e_{pointing}$ is the deviation in the absolute value of the angle between the estimated state and the desired state of the z-axis of reference frame NR, and e_{total} is the net error in the attitude. Note that e_{total} is the quantity of interest for the attitude requirement stated in *Section II*.

This implies that the maximum allowable estimation error to meet the pointing requirements is approximately 0.4 degrees. It is important to note that this is well within the capabilities of the ACS sensors in the heritage Georgia Tech TECHBus design[7].

Figures 6 and 7 show the reaction wheel momenta and the magnetorquer magnetic moments over time. From Figure 6, it is apparent the magnetorquers successfully mitigate momentum buildup in the reaction wheels. Despite the magnetorquers reaching saturation, all pointing requirements and actuator performances are met. If necessary, the magnetorquers can be sized larger to prevent saturation if allowable by power and space constraints.

Figure 8 shows the angular rates of the spacecraft relative to the Earth-Centered Inertial Frame. As expected, the angular rate components in the x- and z- directions are approximately zero while the angular rate component in the y-direction is approximately one revolution per orbit.

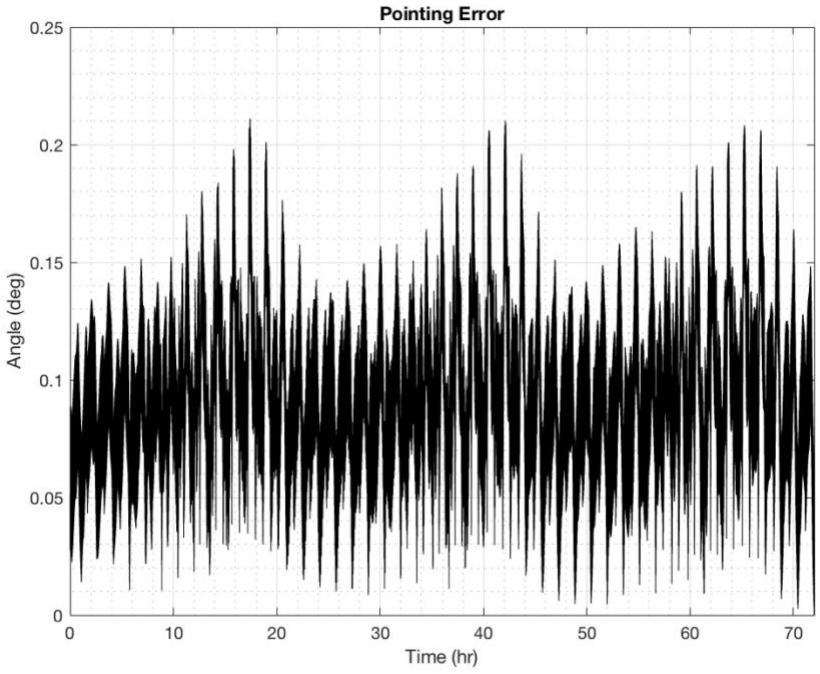

Figure 5. Momentum Wheel Control Scheme – Pointing Error vs. Time

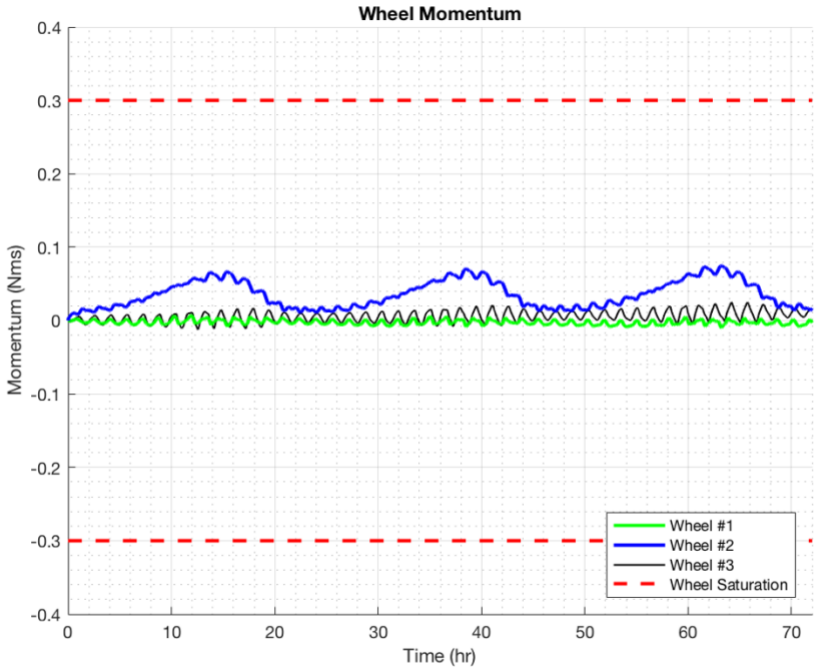

Figure 6. Momentum Wheel Control Scheme – Reaction Wheel Momenta vs. Time

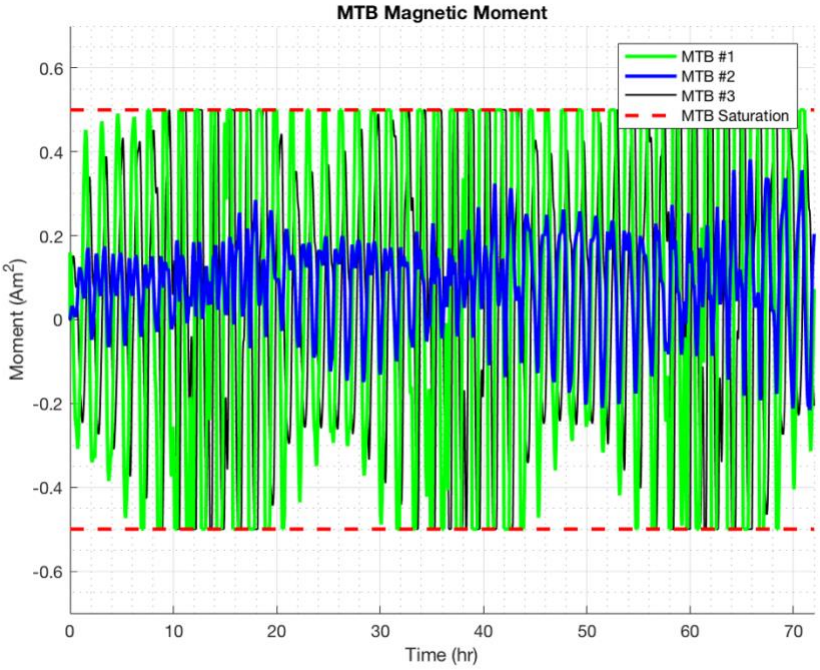

Figure 7. Momentum Wheel Control Scheme – Magnetorquer Magnetic Moment vs. Time

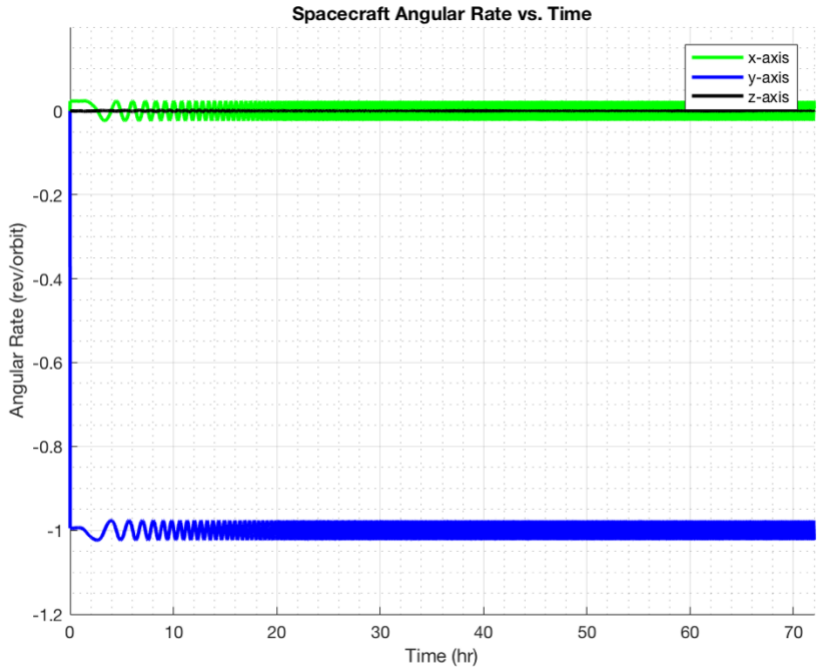

Figure 8. Momentum Wheel Control Scheme – Spacecraft Angular Rates vs. Time

D. Aerotorquer Sizing

Figure 9 compares the required thrust capabilities (for an orbital altitude of 300 km) and the torque required from the thrusters as a function of ${}^{NP}\theta_1^{DP}$, the angle of attack between the spacecraft velocity vector and the y-axis of the aerotorquer. Figure 10 compares the required drag panel area and the torque required from the thrusters as a function of the angle of attack of the aerotorquer for the same orbital altitude of 300 km.

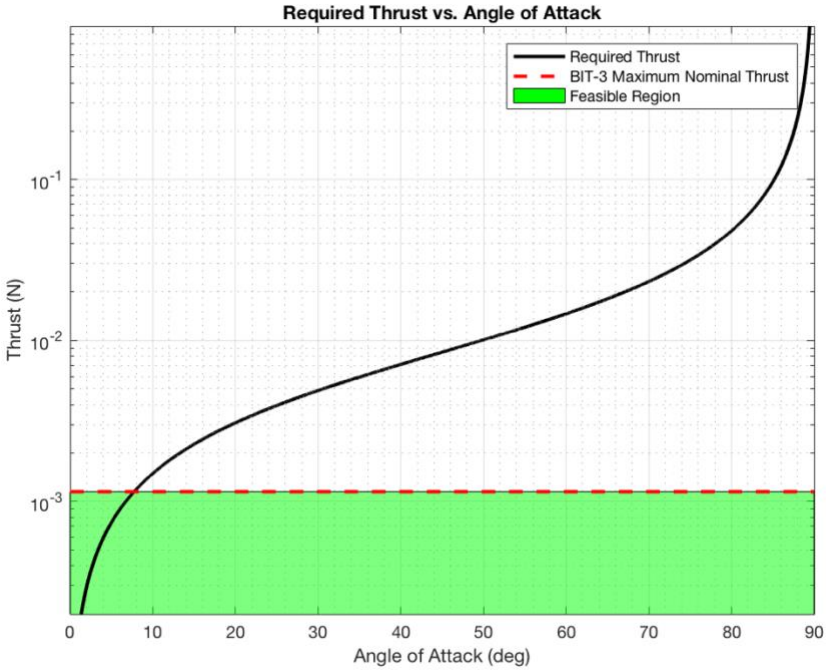

Figure 9. Required Thrust per Ion Thruster vs. Angle of Attack of Aerotorquer (${}^{NP}\theta_1^{DP}$)

As shown in Figure 9, the maximum feasible angle of attack is approximately 7.7°. The corresponding minimum panel area, shown in Figure 10, is approximately 13.5 m^2.

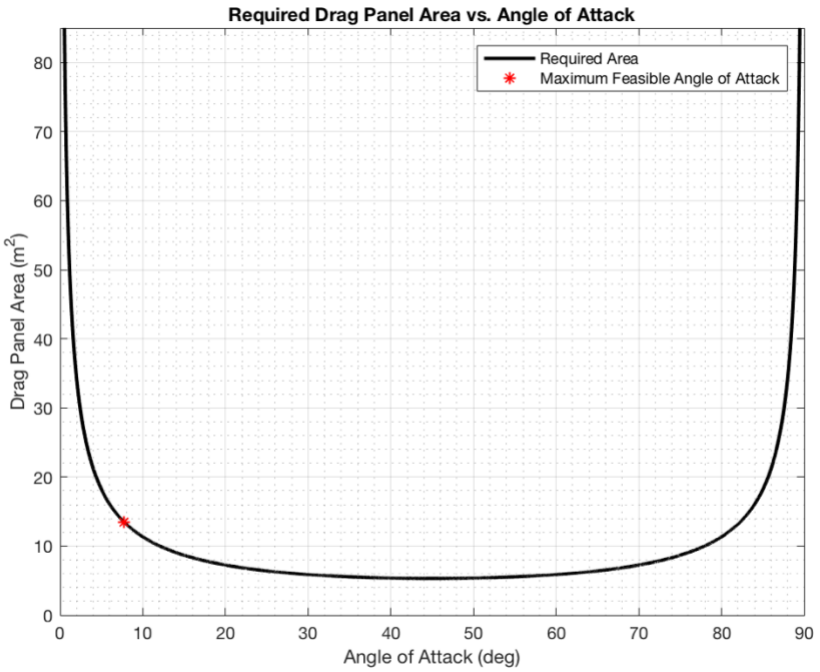

Figure 10. Required Drag Panel Area vs. Angle of Attack of Aerotorquer (${}^{NP}\theta_1^{DP}$)

E. Aerotorquer Control Scheme

Similar to *Section VII, Subsection C*, the aerotorquer control scheme successfully meets the pointing requirements in the presence of a large embedded angular momentum. Figure 11 depicts the pointing performance of the spacecraft. Figures 12 and 13 show the reaction wheel momenta and the magnetorquer magnetic moments over time. Figure 14 shows the angular rates of the spacecraft relative to the Earth-Centered Inertial Frame. Comparing these results to the results of the momentum wheel control scheme, it is clear that once the angular momentum is accounted for, the performance is similar. In the first control scheme, the angular momentum is offset by the momentum wheel. In this control scheme, the aerotorquer and ion thrusters provide a net torque to counteract the angular momentum and ensure a rotation rate near one revolution per orbit. In both control schemes, the reaction wheels provide the fine ACS and the magnetorquers prevent reaction wheel saturation.

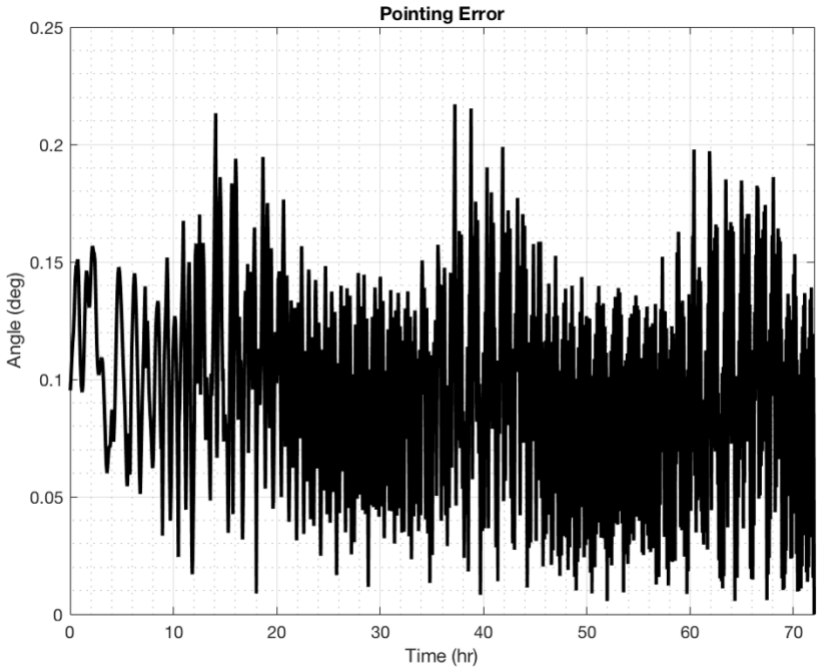

Figure 11. Aerotorquer Control Scheme – Pointing Error vs. Time

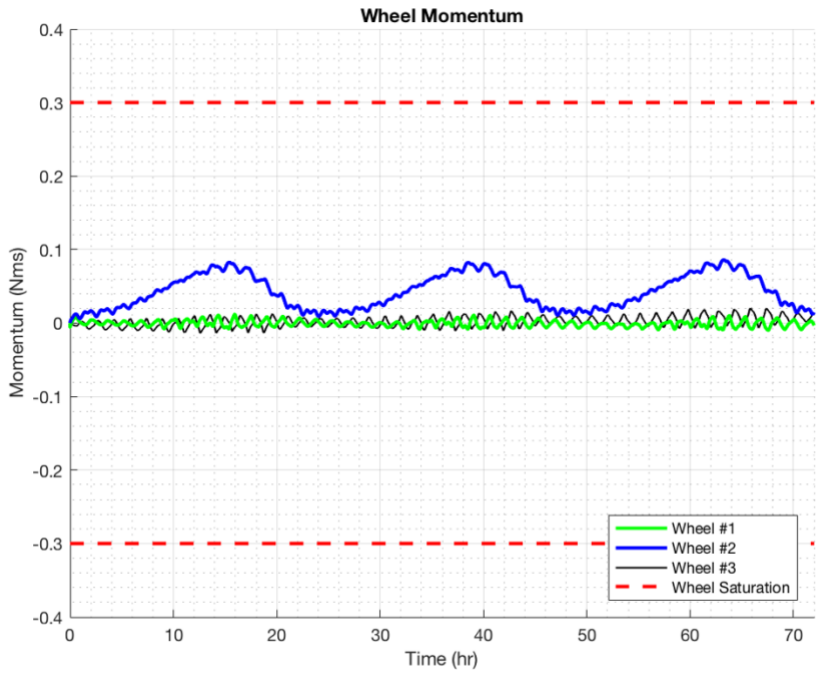

Figure 12. Aerotorquer Control Scheme – Reaction Wheel Momenta vs. Time

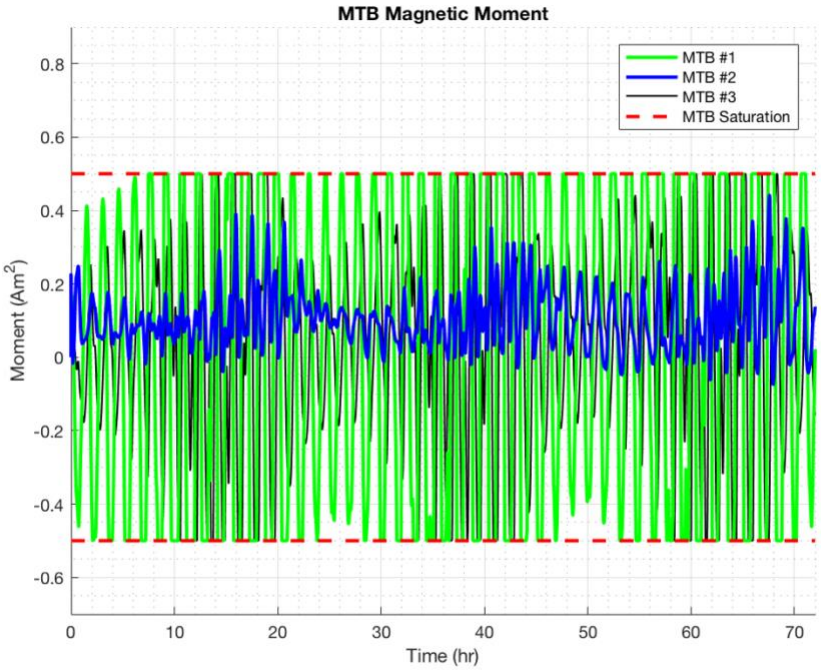

Figure 13. Aerotorquer Control Scheme – Magnetorquer Magnetic Moment vs. Time

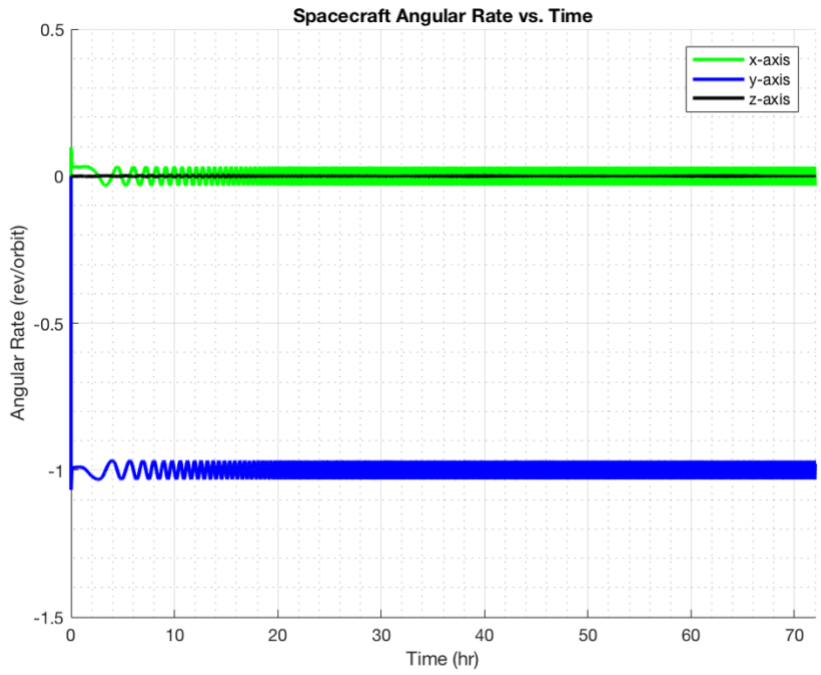

Figure 14. Aerotorquer Control Scheme – Spacecraft Angular Rates vs. Time

VIII. Conclusions

The two ACS designs with the aforementioned control laws successfully stabilize the spacecraft to nadir-pointing while maintaining < 0.5 degree pointing and estimation error. Additionally, the rotation rate of 18 RPM ($\pm$ 0.1 RPM) of the instrument with respect to the LVLH frame is maintained.

Although the aerotorquer control scheme successfully meets the ACS requirements, it is unlikely that this scheme would be feasible or even advantageous for the given problem statement. Assuming a square drag panel and an orbital altitude of 300 km, the required surface area of the drag panel is at least 13.5 m^2. With the space required to stow the drag panel pre-deployment, a momentum wheel could be used instead. If the thrust capabilities of low-thrust thrusters are improved, then the required surface area would decrease making this ACS concept more realistic. Moreover, if the embedded angular momentum requirements are reduced by decreasing the rotation rate and/or the inertia, the required panel area would also decrease.

IX. Future Work

In future analyses, the effect of uncertainty in the inertia parameters on pointing performance of the spacecraft should be studied. Also, realistic sensor models should be added to the simulation to analyze coupling between estimation error and pointing performance.

In this analysis, only passive control using a momentum wheel and an aerotorquer was considered. In future analyses, the angular momentum of the rotating section of the spacecraft should be estimated. In the momentum wheel control scheme, the wheel should be actively controlled to cancel the spacecraft angular momentum. In the aerotorquer control scheme, the torque provided by the aerotorquer should be actively varied via flaps on the drag panel.

Furthermore, the increase in drag due to the aerotorquer will cause significantly faster orbit degradation, which will change the drag produced by the aerotorquer. Therefore, analyses should be performed to validate the performance of the closed-loop aerotorquer controller in the presence of changes to the drag produced by the drag panel. If necessary, an adaptive controller could be applied by treating the atmospheric density as uncertain parameter in the rotational dynamics of the system.

Acknowledgments

This paper was written for AE 8900: MS Special Problems at the Georgia Institute of Technology. First and foremost, I would like to thank my advisor, Prof. E. Glenn Lightsey, for his support and mentorship throughout this research. I would also like to thank Mr. Eric Stoneking of NASA Goddard Space Flight Center for his continued guidance on attitude simulations. Finally, I would like to thank the other students in the Lightsey Research Group – especially William Jun, Terry Stevenson, and Tanish Himani – for their willingness to share ideas and offer suggestions throughout my research.

References

[1]Wise, E. D. (2013). Design, Analysis, and Testing of a Precision Guidance, Navigation, and Control System for a Dual-Spinning Cubesat. Massachusetts Institute of Technology Libraries.

[2]Psiaki, M. L. (2001). Magnetic Torquer Attitude Control via Asymptotic Periodic Linear Quadratic Regulation. Journal of Guidance, Control, and Dynamics, 24(2), 386-394

[3]Li, J., Post, M., Wright, T., & Lee, R. (2013). Design of Attitude Control Systems for CubeSat-Class Nanosatellite. Journal of Control Science and Engineering, 2013, 1-15

[4]Neilsen, Tim; Weston, Cameron; Fish, Chad; and Bingham, Bryan, "Dice: Challenges of Spinning Cubesats" (2014). Space Dynamics Lab Publications. Paper 97.

[5]Wise, E. D., Pong, C. M., Miller, D., Cahoy, K., & Nguyen, T. T. (2013). A Dual-Spinning, Three-Axis-Stabilized CubeSat for Earth Observations. AIAA Guidance, Navigation, and Control (GNC) Conference

[6]The Aerospace Corporation, Rowen, D., & Dolphus, R. (2013). 3-Axis Attitude Determination and Control of the AeroCube-4 CubeSats. Presentation presented at The Aerospace Corporation.

[7]Francis, P., "Development of the Evolved Common Hardware Bus," Master's Thesis, Guggenheim School of Aerospace Engineering, Georgia Tech, Atlanta, GA, 2016.